Materials Science & Engineering C 106 (2020) 110143

Contents lists available at ScienceDirect

Materials Science & Engineering C

journal homepage: www.elsevier.com/locate/msec

Poly-L-arginine modifications alter the organization and secretion of collagen in SKH1-E mice

Anuraag Boddupalli[a], Dana Akilbekova[b,1], Kaitlin M. Bratlie[a,b,c,*]

[a] Department of Chemical & Biological Engineering, Iowa State University, Ames, IA 50011, United States of America
[b] Department of Materials Science & Engineering, Iowa State University, Ames, IA 50011, United States of America
[c] Division of Materials Science & Engineering, Ames National Laboratory, Ames, IA 50011, United States of America

ARTICLE INFO

Keywords:
Second harmonic generation
SHG
Collagen
SKH1-E mouse
Poly-L-arginine

ABSTRACT

Functionalized biomaterials interface with tissue upon implantation. There is a growing need to understand how materials properties influence this interaction so that efficient tissue engineering systems can be developed. In this study, we characterize collagen organization in response to functionalized glass beads implanted in SKH1-E mice. Poly-L-arginine (PLR) was modified with arginine derivatives to create a functionalized surface and was coated on glass beads. Tissue sections were removed 28 days post-implantation and were imaged using second harmonic generation (SHG) microscopy. These chemical modifications were able to alter the collagen distribution from highly aligned to disordered (17 ± 6 to 78 ± 1° full width at half-maximum (FWHM)) and the collagen III/I ratio (0.02 to 0.42). Principal component analysis (PCA) comparing the physical properties of the modifiers (*e.g.* hydrophobicity, molar volume, freely rotating bonds, polarizability) with the SHG analytically derived parameters (*e.g.* collagen III/I ratio, collagen orientation) was performed. Chemical properties of the PLR-like modifications including lipophilicity, along with the number of freely rotating bonds and the polarizability had significant effects on the collagen surrounding the implant, both in terms of collagen orientation as well as the production of collagen III. These findings demonstrate the possibility of tuning the foreign body response, in terms of collagen deposition and organization, to positively influence the acceptance of implanted biomaterials.

1. Introduction

The foreign body response is a complex series of processes initiated upon implantation of a biomaterial. The affected tissue responds to the implant through the secretion of chemokines, cytokines, and matrix metalloproteinases in an attempt to restore normal function at the implant site [1]. Different cell types participate in the foreign body response with specific roles as the tissue seeks to halt blood flow and repair the damaged extracellular matrix (ECM) [2,3]. The foreign body response interferes with the cascade of cell signaling pathways involved in normal wound closure by extending the inflammatory response phase [4]. This hindered the wound healing response to the implant consists of protein adsorption on the implant surface, recruitment of monocytes, monocyte differentiation into macrophages, macrophage fusion into foreign body giant cells, differentiation and activation of fibroblasts to myofibroblasts, and fibrotic encapsulation [5]. Post inflammation fibroblasts and myofibroblasts secrete collagen, particularly types I and III, in the case of dermal tissues to synthesize a fibrotic layer in response to the implant. The organization of collagen in this fibrous collagen-rich layer can vary from well-aligned to a stochastic distribution of collagen fibrils [6]. These deposited collagen fibrils become active components of the basement membrane reconstruction, by promoting the attachment of endothelial cells [2]. During the remodeling phase of wound healing, collagen fibers are aligned stochastically similar to that of unwounded tissues [7]. Healed tissues often do not recover their full mechanical strength, regaining only around 80% of the levels prior to the tissue damage [8]. Scar tissue or incompletely healed tissue contain bundles of organized collagen fibers, compared to the isotropic organization in undamaged tissue [9]. In scar tissue, collagen type III is replaced by fibrillar collagen type I, as observed in fibrotic capsules surrounding implant sites [10]. Isotropic collagen orientation with similar levels of collagen III as that in healthy dermal tissues, would be the ideal collagen response to implanted biomaterials [11].

* Corresponding author at: Department of Chemical & Biological Engineering, Iowa State University, Ames, IA 50011, United States of America.
E-mail address: kbratlie@iastate.edu (K.M. Bratlie).
[1] Current address: School of Engineering, Chemical Engineering Department, Nazarbayev University, Astana, Kazakhstan.

https://doi.org/10.1016/j.msec.2019.110143
Received 28 March 2018; Received in revised form 23 August 2019; Accepted 27 August 2019
Available online 02 September 2019
0928-4931/

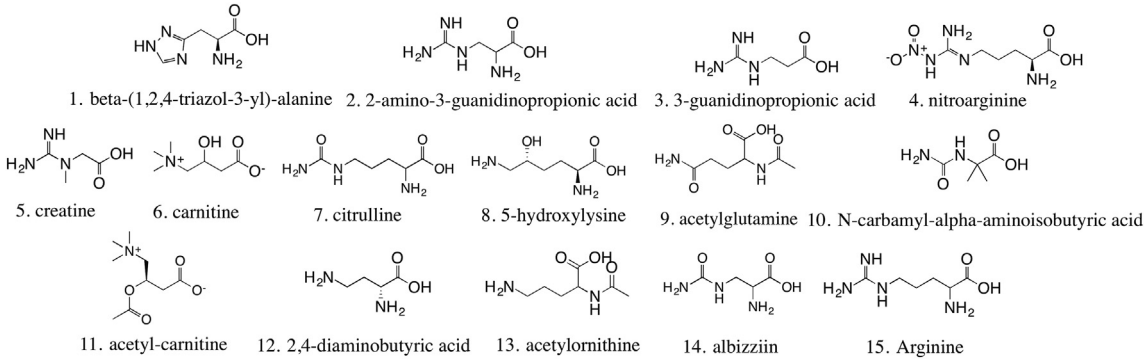

Fig. 1. Chemical structures of the molecules used in the modification of poly-L-arginine (PLR). The arginine derivatives shown here are numbered for easier identification in experiments and discussion throughout the paper.

Multimodal imaging techniques such as second harmonic generation microscopy (SHG) enable sensitive, dye-free imaging of collagen in various clinical samples [12]. In this non-linear microscopy process, two photons of the same wavelength are impinged spatially and temporally on a sample. When these photons interact with non-centrosymmetric moieties, they double in frequency [13]. The non-centrosymmetric chemical structure of collagen arising from its triple helical structure, make it an SHG-active biomolecule. Changes in collagen density, organization, and type can be determined using SHG analysis. Other biomolecules that have been imaged using SHG are myosin in muscle tissue and cholesterol crystals in atherosclerotic plaques [14,15].

SHG microscopy of triple helical collagen fibers can provide more information about the collagen response through susceptibility tensor analysis [12,16]. These parameters are linked to the materials properties, based on the molecular origins of the collagen signal arising from the ratio of their methylene to peptide bonds [17]. Polarization resolved SHG microscopy is capable of differentiating between diverse types of collagen in dermal samples by generating a map of the susceptibility tensor components. Specifically, the ratio of collagen types I and III can be estimated by analyzing the ratio of the nonlinear susceptibility tensor elements [12]. Collagen type I is significantly more prevalent than type III in human skin, and the ratio of III/I is ~30% for unwounded adult dermis [18]. As wound healing progresses, this ratio can rise to ~90% and gradually decreases during the re-epithelialization process [19]. Elevated levels of collagen type III are linked to a prolonged wound healing process. In some cases, these elevated levels are associated with hypertrophic scarring or internal injuries such as inguinal hernia [10,19,20]. However, there is no consensus on the role played by collagen type III on the wound healing process, or the biomaterials properties that can induce different levels of collagen type III. It has been observed that as wound healing progresses towards the granulation phase, collagen I is replaced by collagen III particularly for tissues that undergo significant mechanical stress, which indicates a difference in mechanotransductive signaling roles in the two types of collagen in the ECM [21]. This change in significant tissue strength for higher collagen III is also observed for tissues prone to developing different types of hernias [19]. During scar tissue formation, collagen type III is organized with collagen type I in aligned bundles whereas they are stochastically arranged in healthy tissue [11].

Our study focuses on analyzing the collagen response to functionalized glass beads implanted in SKH1-E mice. These mice are commonly used for studying dermal wound healing responses as they are hairless, making application and observation of topical treatments relatively easy [22]. We used a library of chemical modifiers based off the amino acid arginine and its derivatives, which have been previously shown to influence the synthesis of collagen by fibroblasts *in vitro* [23], to examine how materials properties alter collagen organization. In another study examining collagen responses to materials, functionalized polystyrene microparticles were examined and it was found that dimethylamino functionalized particles resulted in isotropic collagen organization and a thin fibrotic capsule [6]. Poly-L-arginine (PLR) modified with arginine derivatives and coated on glass beads showed the influence of collagen directionality on the speed of fibroblast migration and secretion of angiogenetic cytokines such as vascular endothelial growth factor [24]. The metabolism of L-arginine by immunologically relevant cells like macrophages and fibroblasts affects diverse outcomes including wound healing [25,26] and tumor progression [27] through their effect on the rate of synthesis of collagen [28,29]. Furthermore, arginine derivatives such as nitroarginine [30] and acetylcarnitine [31] have been studied for their effect on damaged neurons protecting them from membrane damage as well as microglial activation [32]. With these insights on the influence of arginine and its' derivatives on immune response, we have uncovered physicochemical properties of these materials that correlate with collagen organization and the ratio of collagen type III/I. Analyses such as these aim to improve rational design for biomaterials that can tune the fibrotic response towards better implant acceptance.

2. Materials and methods

Experiments were performed with a minimum of three replicates. Results were compared to controls of unmodified PLR and uncoated glass beads. All materials were purchased from Sigma (St. Louis, MO) and used as received, unless otherwise indicated. Fresh deionized (DI) water (Milli-Q Nanopure, Thermo Scientific, Waltham, MA) and sterile 1× phosphate buffered saline (PBS, diluted from 10× solution (Fisher, Pittsburgh, PA), to 0.1 M, pH 7.4) was used throughout this study.

2.1. Materials

Surface modifiers were coupled to 29,000 Da PLR (Alamanda Polymers, Huntsville, AL). These modifiers are shown in Fig. 1 and include β-(1,2,4-triazol-3-yl)-alanine, 2-amino-3-guanidinopropionic acid (Matrix Scientific, Elgin, SC), 3-guanidinopropionic acid, nitroarginine, creatine (Acros Organics, Pittsburgh, PA), carnitine, citrulline, 5-hydoxylysine, acetylglutamine, N-carbamyl-α-aminoisobutyric acid, acetyl-carnitine, 2,4-diaminobutyric acid, acetylornithine, albizziin, and arginine (Amresco, Solon, OH).

2.2. PLR modification

The fifteen different modifiers (Fig. 1) were coupled to PLR using 1-ethyl-3-(3-dimethylaminopropyl)carbodiimide (EDC, Oakwood Chemical, West Colombia, SC). These materials were modified as previously described [24] using 4 mL of a 2.5 mg/mL solution of PLR in phosphate buffered saline (PBS) with 100 M equivalents of arginine derivative. EDC (200 mg) was added to the scintillation vial and stirred

for 4 h at room temperature. The modified polymers were dialyzed against H_2O for 24 h and subsequently lyophilized (4.5 L, Labconco, Kansas City, MO). The modified PLR was re-suspended in PBS at 0.1% w/v and stored at −20 °C.

2.3. Ethics statement

The research protocol was approved by the local animal ethics committees at Iowa State University (Institutional Animal Care and Use Committee) prior to initiation of the study.

2.4. Animals

Female SKH1-E mice (6-weeks old) were obtained from Charles River Laboratories (Wilmington, MA). The mice were maintained at the animal facilities in the College of Veterinary Medicine at Iowa State University, accredited by the American Association of Laboratory Animal care, and were housed under standard conditions with a 12-hour light/dark cycle. Both water and food were provided *ad libitum*.

2.5. Subcutaneous injections

Animal tissue specimens previously obtained [24] were used here. Briefly, injections were performed according to ISO 10993-6:2007. Glass beads (105–150 μm, Warrington, PA) were sterilized *via* autoclave and were coated with each of the fifteen modified PLRs, PLL (poly-L-lysine), and unmodified PLR. Uncoated glass beads were also tested. Mice were anesthetized *via* isoflurane inhalation at a concentration of 1–4% isoflurane/balance O_2 to minimize movement. The backs of the mice were scrubbed with 70% isopropyl alcohol and five modified glass beads (10% v/v, 100 μL) were injected in an array format with a sixth injection of unmodified PLR coated beads. All experiments were conducted in quintuplicate. After 28 days, the mice were euthanized *via* CO_2 asphyxiation. The injected beads and surrounding tissue were excised. Sections were fixed in 10% formalin, embedded in paraffin, sectioned into 5 μm slides, and mounted on glass slides.

2.6. Collagen gel preparation

Collagen type I (BD Biosciences, Franklin Lakes, NJ) was solubilized in acetic acid (20 mM) at 10 mg/mL to prepare a stock solution. This solution was mixed on ice with 10 × PBS, 1 M NaOH and deionized water to prepare aliquots of 1, 2, 4 and 6 mg/mL of collagen type I solutions. This solution was then pipetted on to glass coverslips and gelled at 37 °C for 1 h.

2.7. Second harmonic generation (SHG)

The laser system is a mode-locked Ti:sapphire laser (100 fs pulse width, 1 kHz repetition rate, Libra, Coherent, Santa Clara, CA) that produces an 800 nm fundamental. The average power at the samples was kept at 1–10 mW using a half-wave plate and a Glan-Thompson polarizer (Thorlabs, Newton, NJ) to avoid tissue damage. SHG images were collected in transmission mode. An inverted microscope stage (AmScope, Irvine, CA) and a 20× Nikon Plan Fluorite objective (0.50 NA, 2.1 mm) were used to focus the 800 nm beam. The second harmonic signal was collected with a 40× Nikon water immersion objective (0.8 NA, 3.5 mm). The signal was reflected with a dichroic mirror (Thorlabs) and the fundamental beam was removed using a short pass filter < 450 nm (Thorlabs) and an 808 nm notch filter (Melles Griot, Rochester, NY). The signal was detected using an intensified charge-coupled device camera (iCCD, iStar 334 T, Andor, Belfast, UK) with 512 × 512 active pixels. The polarization of the incoming beam was changed using a Glan-Thompson polarizer and a half-wave plate mounted on a motor driven rotational stage (Thorlabs). These optics were inserted before the focusing objective.

Images of tissue sections and collagen standard curve samples were collected every 10° from 0 to 350°. Final images were acquired by averaging at least 15 images for each polarization angle. A minimum of three sets of polarization images for each experimental condition were taken. Birefringence was calculated to be within the resolution of the polarization angles for the thickness of tissues (5 μm) used in this study.

2.8. Image processing

The intensity of the second harmonic signal of collagen as a function of polarization angle of the incident laser beam can be written as:

$$I_{SHG} = c.\left\{\left[\sin^2(\theta_e-\theta_o)+\left(\frac{\chi_{zzz}}{\chi_{zxx}}\right)\cos^2(\theta_e-\theta_o)\right]^2+\left(\frac{\chi_{xzx}}{\chi_{zxx}}\right)^2 \sin^2(2(\theta_e-\theta_o))\right\} \quad (1)$$

where $\frac{\chi_{zzz}}{\chi_{zxx}}$ and $\frac{\chi_{xzx}}{\chi_{zxx}}$ are second-order susceptibility tensor element ratios; θ_e and θ_o are the incident polarization angle and collagen fiber angle, respectively; and c is a normalization constant. Tensor elements can be used as a contrast mechanism for distinguishing sources of SHG signal [6,33]. Images were filtered using a median noise filter (3 × 3) to attenuate the salt and pepper noise in the acquired images (ImageJ, NIH, Bethesda, MD). Images were binned to obtain regions of interest (ROIs) of 2 × 2 pixels. Collagen orientation angles and second-order susceptibility tensor element ratios were determined for every ROI by fitting to a Levenberg-Marquardt algorithm using Matlab (MathWorks, Natick, MA). Photon counts below 5 counts per pixel were excluded from the analysis as this was determined to be below the limit of detection for this setup. The limit of detection was determined by measuring ambient noise detected by the iCCD when the incoming light was blocked. The Matlab script generated images displaying the orientation angles of collagen determined for each ROI and heat maps for the second-order susceptibility tensor element ratios. Histograms for both were also obtained.

2.9. Statistics and data analysis

Statistical analysis was performed using JMP® statistical software (Cary, NC). Statistical significance of the mean comparisons was determined by a two-way ANOVA. Pair-wise comparisons were analyzed with Tukey's honest significant difference test. Differences were considered statistically significant for $p < 0.05$. Principal component analysis (PCA) was conducted to explain relationships between modifier properties and experimentally derived parameters. The principal components were calculated as linear combinations of the plotted parameters, to denote the directions of maximum variance. The correlations between different properties can be observed as projected values against the two principal components (PC1 and PC2).

3. Results

3.1. Collagen signal

SHG imaging of the collagen response to the different PLR modifications was conducted to qualitatively evaluate the differences. (Fig. 2), Collagen signal was measured and compared against a standard curve of collagen concentration *versus* SHG signal intensity which was fit using the equation below (R^2 = 0.99, Fig. 3A).

$$I_{SHG} = -7.75 \times 10^5 x^2 + 3.14 \times 10^7 x \quad (2)$$

where x is the collagen concentration in mg/mL.

There were no significant differences in the amount of collagen

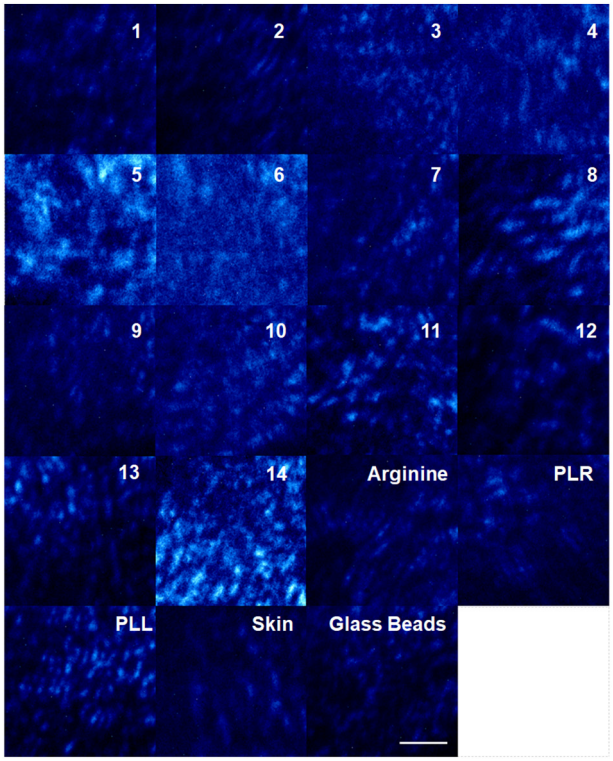

Fig. 2. Representative SHG images of collagen response surrounding implanted glass beads coated with modified PLR. The SHG intensity is in blue pseudocolor, and the scale bar represents 20 μm. (For interpretation of the references to colour in this figure legend, the reader is referred to the web version of this article.)

present in 16 of the 18 modifications tested *ex vivo* (Table 1). The collagen signal in response to the creatine and albizziin modifications were ~2-fold higher than the control samples of naïve glass bead and untreated skin samples (Fig. 3B).

3.2. Collagen organization

The collagen organization was quantified by fitting the obtained histograms with Gaussian curves (Fig. 4). Using the full-width at half-maximum (FWHM) values of the Gaussian fits, there were clear differences for some modifiers (Table 1). Collagen organization in response to modifications carnitine (Mod 6), 5-hydroxylysine (Mod 8), acetylcarnitine (Mod 11), albizziin (Mod 14), Poly-L-lysine (PLL), and arginine (Mod 15) was relatively isotropic. The isotropy for these modifications was confirmed by an algorithm referred to as an isotropy check, given below as Eq. (3). The confidence interval was subtracted from the peak of the Gaussian fit of the histograms and if this peak was 125 points greater than the average plus the confidence interval, the peak was considered a false value.

$$If\ [Height - CI_{Height}] > [\ Average + CI_{Average} + 125] \quad (3)$$

$$Then\ Collagen\ Organization = Isotropic$$

This algorithm was applied to modifications where the peaks arose from only one or two bins with the remaining bins being statistically similar. The FWHM for the nitroarginine modification (25 ± 4°) showed highly aligned collagen organization whereas organization for the arginine modification was relatively isotropic and failed the isotropy check test. Comparisons of citrulline (55 ± 11°) to albizziin (isotropic organization) and 2-amino-3-guanidinopropionic acid (55 ± 10°) to arginine (isotropic organization) modifications showed clear differences in collagen response. Interestingly, these modifications have similar chemical structure with the exception that citrulline and arginine contain two additional CH_2 groups, compared to their albizziin and 2-amino-3-guanidinopropionic acid counterparts with contradictory trends for collagen isotropy. The most aligned collagen response was observed for N-carbamyl-α-aminoisobutyric acid (15 ± 3°) while the 3-guanidinopropionic acid modification elicited the widest, recognized (based on the isotropy check) collagen organization with a FWHM of 78 ± 1°. The area under the curve was tabulated from the orientation angle curve fits (Table 1). The area under the curve was significantly higher for the citrulline modification (15,099 ± 3508), compared to the response of all other modifications.

3.3. Collagen III secretion

The nonlinear susceptibility tensor ratios were calculated for each ROI and were plotted as histograms (Fig. 5), which were then used to estimate the collagen III presence. A gradient curve previously obtained [6] for collagen III concentration was used to estimate the collagen III/I ratio, thus enabling comparisons of the type of collagen deposited surrounding the different chemical modifications (Table 1). Nitroarginine (36 ± 8%) resulted in almost twice the amount of collagen III surrounding the implant compared to arginine (18 ± 3%). As noted

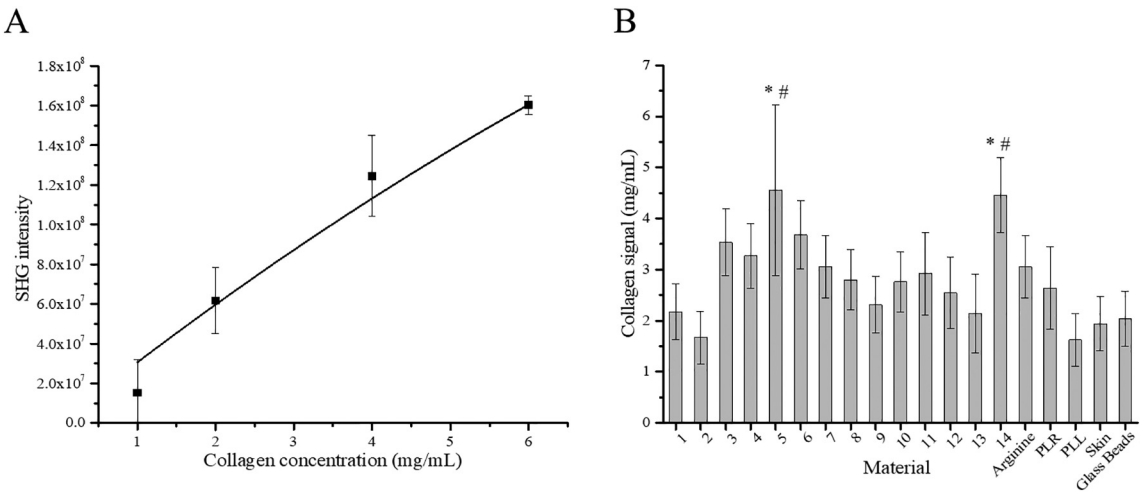

Fig. 3. Quantification of collagen surrounding implanted glass beads coated with modified PLR. (A) Standard curve for collagen type I concentration. The SHG intensity is plotted against the known concentration of collagen concentration. (B) Quantification of collagen concentration surrounding implants. Data represents the mean ± standard deviation (SD). $n = 5$. Statistical analysis through two-way ANOVA and Tukey's HSD post-hoc test. $^*p < 0.05$.

Table 1
Approximated collagen concentration, collagen type III ratio, organization (measured as FWHM) and area under the organization curve fitting for the collagen response surrounding implanted glass beads coated with modified PLR. Data represents the mean ± standard error. n = 5.

S no.	Modification	Collagen signal (in mg/mL)	Collagen III ratio	FWHM	Area under the curve
1	β-(1,2,4-triazol-3-yl)-alanine	2.17 ± 0.54	0.16 ± 0.04	17 ± 2	4530 ± 562
2	2-amino-3-guanidinopropionic acid	1.67 ± 0.51	0.18 ± 0.04	55 ± 10	6229 ± 1306
3	3-guanidinopropionic acid	3.53 ± 0.65	0.19 ± 0.05	78 ± 1	7127 ± 984
4	Nitroarginine	3.27 ± 0.63	0.36 ± 0.08	25 ± 4	9298 ± 1382
5	Creatine	4.56 ± 0.75	0.05 ± 0.02	16 ± 3	4646 ± 794
6	Carnitine	3.68 ± 0.66	0.05 ± 0.01	–	–
6	Citrulline	3.06 ± 0.61	0.02 ± 0.01	55 ± 11	15,099 ± 3508
7	5-hydroxylysine	2.80 ± 0.59	0.16 ± 0.03	–	–
8	Acetyl glutamine	2.31 ± 0.55	0.08 ± 0.02	17 ± 6	2222 ± 728
9	N-carbamyl-α-aminoisobutyric acid	2.76 ± 0.59	0.07 ± 0.01	15 ± 3	3608 ± 868
10	Acetylcarnitine	2.92 ± 0.81	0.10 ± 0.03	–	–
11	2,4-diaminobutyric acid	2.54 ± 0.70	0.09 ± 0.02	23 ± 5	3080 ± 634
12	Acetylornithine	2.14 ± 0.77	0.09 ± 0.01	19 ± 4	4299 ± 880
13	Albizziin	4.46 ± 0.74	0.42 ± 0.13	–	–
14	Arginine	3.05 ± 0.61	0.18 ± 0.03	–	–
	Poly-L-arginine	2.64 ± 0.81	0.21 ± 0.03	29 ± 3	7773 ± 862
	Poly-L-lysine	1.62 ± 0.51	0.07 ± 0.03	–	–
	Skin	1.94 ± 0.53	0.26 ± 0.07	41 ± 5	9292 ± 1085
	Glass Beads	2.04 ± 0.54	0.14 ± 0.04	24 ± 2	7696 ± 723

above, collagen surrounding the nitroarginine modification was significantly more aligned than the isotropic collagen surrounding the arginine modification. In comparing the 2-amino-3-guanidinopropionic acid and arginine modifications, which differ by two CH_2 groups, the fiber organization was significantly different, with the former being more oriented. In contrast, both modifications resulted in similar levels of collagen type III surrounding the implant (18%, $p > 0.05$). In the case of albizziin and citrulline modifications, citrulline was produced more aligned collagen than albizziin and resulted in twenty times less collagen type III than albizziin (2 ± 0% for citrulline and 42 ± 13% for albizziin) surrounding the implant. Citrulline has two additional CH_2 groups separating the urea and amine functional groups than albizziin. The PLL coating resulted in a third the amount of collagen type III (7 ± 3%) surrounding the implant compared to the PLR coating (21 ± 3%). Converting the urea functional group on albizziin to a guanidine (2-amino-3-guanidinopropionic acid) resulted in a two-fold decrease in the collagen type III levels in the neighboring tissue.

3.4. Statistical analysis

The correlation matrix (Table S1), and the PCA (Fig. 6) were used to explain relationships between the experimentally observed second harmonic parameters and the chemical properties of the modifiers. Freely rotating bonds (r) of the modifiers was correlated ($R = 0.47$, Table S1) with the FWHM of the collagen orientation. There were also correlations for the collagen III ratio with surface tension and the hydrogen bond acceptors (HBA) of the modifiers ($R = 0.72$ and 0.62, respectively). Based on the PCA of the collagen organization with the properties of the modifiers (Fig. 6), the lipophilicity (LogD at pH 5.5), surface tension, and the number of HBA of the chemical modifier were correlated to the collagen III levels.

Previously obtained cell responses to these PLR modifications [6] were also analyzed using PCA to uncover additional correlations. The speed of the cell migration on PLR modified surfaces was negatively correlated with polarizability ($R = -0.53$) and molar volume ($R = -0.50$), while having a positive correlation with log P ($R = 0.48$) of the modifiers (Table S1). The persistence of the cells in response to the modifiers was found to correlate positively to log D at pH 5.5 ($R = 0.58$).

4. Discussion

Collagen organization and type are indicators of implant acceptance as well as the stage of the wound healing process. Collagen is secreted and remodeled by stromal cells such as fibroblasts and myofibroblasts to promote wound contraction [34]. SHG microscopy is a high information, dye-less, non-linear optical technique that can visualize collagen organization and type in diverse tissues [6,16,35]. Our previous research on examining the isotropy of collagen yielded insight into the combinations of arginine and its derivatives that can be used to direct organization of the stroma. In this study, we further examine how chemical modifications alter collagen organization, rational design of biomaterials can be improved.

4.1. Collagen signal comparisons

The collagen signal for the 18 different modifications was estimated to be in the range of 2 to 5 mg/mL. Modification 5 (creatine) resulted in significantly higher collagen secretion at an estimated 4.56 ± 0.75 mg/mL, almost twice that of the control skin sample (1.94 ± 0.53 mg/mL). Creatine is a stimulant for promoting collagen secretion by fibroblasts in dermal tissues [36]. In another study, creatine supplements were observed to significantly increase skin firmness through stimulating procollagen secretion and collagen alignment in young and aged humans, which was measured *in vivo* using multiphoton laser scanning microscopy [37]. The effect of the PLR-like modifications on the differentiation of fibroblasts associated with collagen synthesis and the wound healing response showed that it is possible to tune the modifier's chemical properties to enhance angiogenesis related biomarkers such as vascular endothelial growth factor [24]. Statistical analysis on the chemical structure of the modifier and its influence on *in vivo* collagen organization indicated the modifier's hydrophobicity was positively correlated to the collagen type III deposition. Studies on collagen organization in response to chemical modifications are uncommon, and there is a growing need to elucidate the materials properties responsible for collagen deposition and organization during the foreign body response. It is important to note here that there are limitations in SHG-based collagen sensing as well, deriving from the limited z-axis depth of imaging, as well as significant differences arising from imaging fibrillar and non-fibrillar sources of collagen [38].

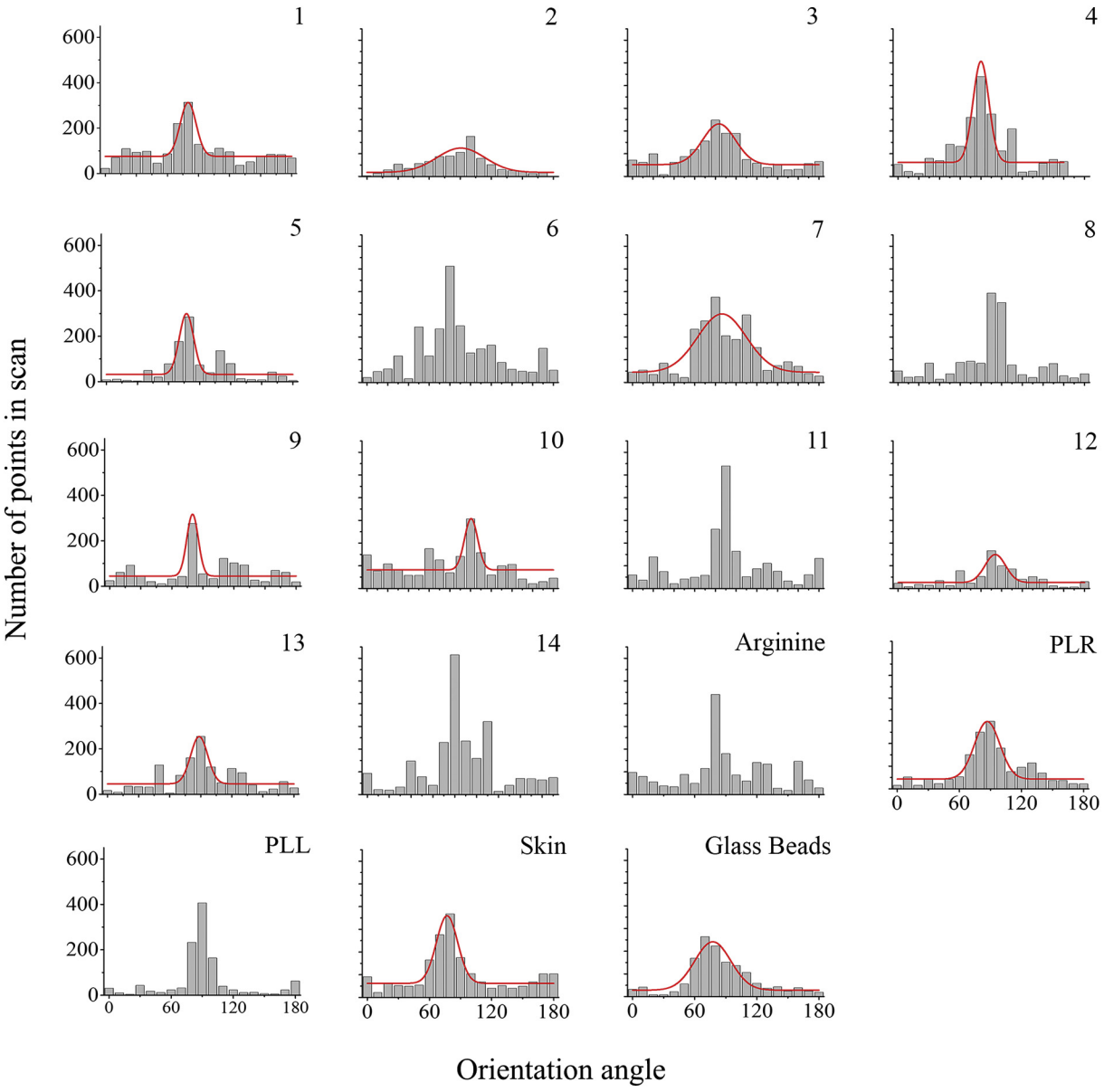

Fig. 4. Histograms of collagen organization surrounding implanted glass beads coated with modified PLR. The bars represent experimentally acquired data. The red line is the Gaussian fit to the data. (For interpretation of the references to colour in this figure legend, the reader is referred to the web version of this article.)

4.2. Collagen organization response

Collagen organization in response to *in vivo* implantation of PLR modified glass beads was quantified using the FWHM, area under the fit, and skewness and kurtosis of the curve fit (Fig. 4). For modifications that failed the isotropy check test, it was qualitatively observed that there was a relatively consistent amount of collagen imaged between 0 and 180°, with the presence of a few bins that were causing over-fitting of the histogram. In Table 1, the FWHM and area under the curve for these histograms have been removed.

There was an inconsistent trend for carbon chain length with collagen organization. Citrulline and albizziin have almost the same chemical structure, with the former having a $–CH_2$ group making its chain length longer. Similarly, arginine has the longer chain with otherwise similar chemical structure as compared to amino-3-guanidinopropionic acid modification. The comparison of the collagen organization response to albizziin and citrulline was interesting as the former is longer in chain length, and had a relatively aligned collagen response, with the shorter chain length containing albizziin resulting in an isotropic one. However, this trend was not continued for the case of comparing the shorter 2-amino-3-guanidinopropionic acid (aligned collagen response) to the longer modification of arginine (isotropic collagen response). There was also no consistent trend for the other modifications that elicited isotropic collagen organization responses. These observations support the hypothesis that collagen organization in response to implanted biomaterials is a complicated process, which cannot be readily mapped on the basis of purely chemical structure comparisons of the modifications.

Unwounded dermal tissue contains disordered collagen and is considered a marker for implant acceptance [39]. Studies have shown that disordered collagen organization in dermal tissues is significantly different from the heavily aligned conformations shown for scarring and hypertrophic lesions [40]. There are clear differences in collagen organization even between different types of scarring (*e.g.*, keloids and hypertrophic scars), which can be similar to the fibrotic responses to rejected implants [9]. SHG analysis of aligned collagen fiber responses can assess ECM organization, which is a marker that can lead to failure of implanted biomaterials [6,41]. In specific cases, it becomes vital to

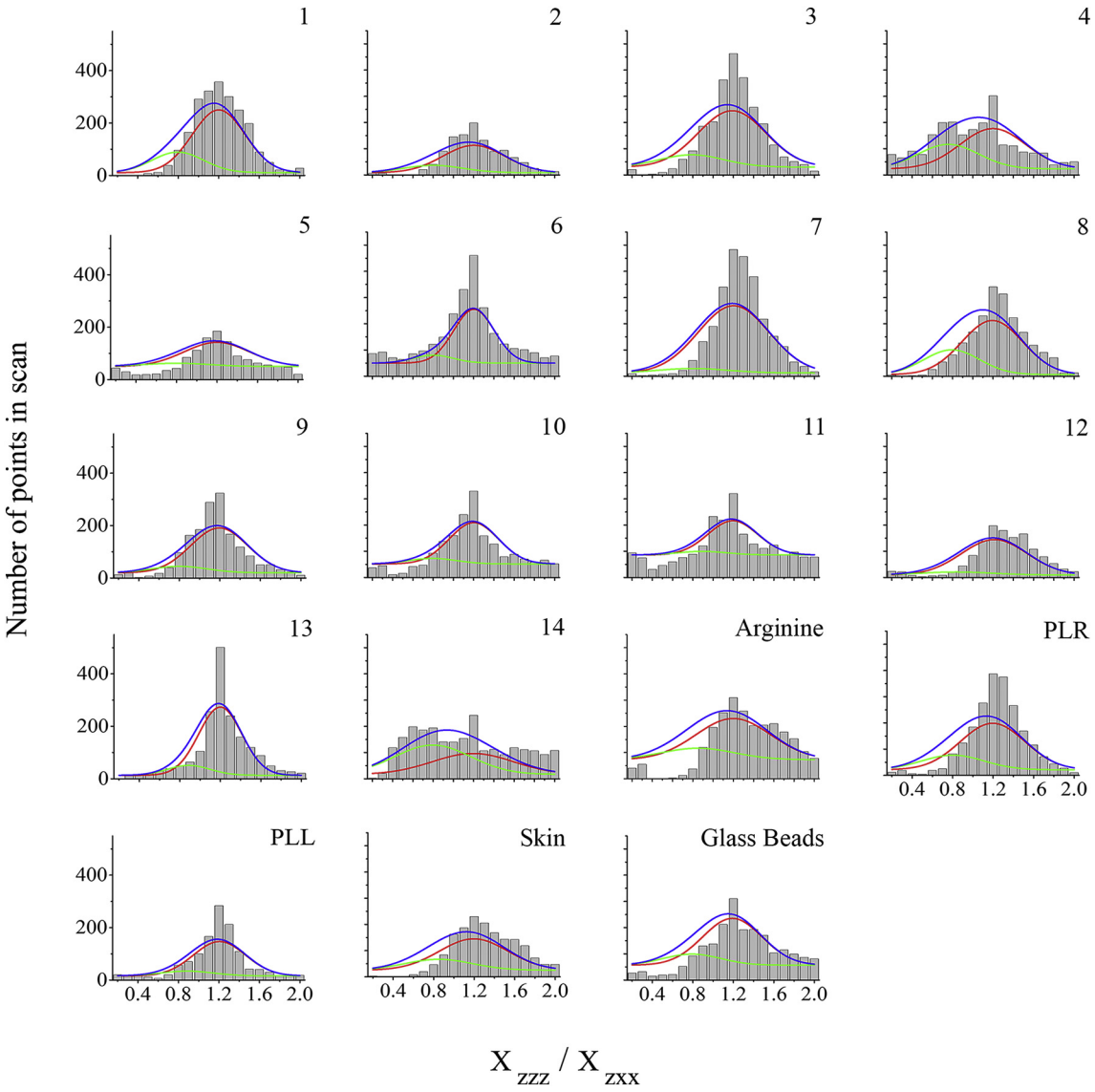

Fig. 5. Histograms of $\frac{\chi_{zzz}}{\chi_{zxx}}$ values obtained for implanted glass beads coated with modified PLR. The bars represent experimentally acquired data. The blue line is the bimodal Gaussian fit to the data. The individual modes are represented as green (collagen type III) and red (collagen type I) lines. (For interpretation of the references to colour in this figure legend, the reader is referred to the web version of this article.)

increase the alignment of collagen fibers to mimic unwounded conditions such as in the knee meniscus [42]. In another study, cell seeding density had an influence on collagen secretion and subsequent alignment in response to mechanical cues for the formation of neocartilage in soft hydrogels [43]. Tuning collagen organization thus plays a key role in the foreign body response [5] and wound healing [24].

4.3. Collagen III response

Secretion of collagen III is observed early in the wound healing process, with continued elevated levels of collagen III/I ratios indicating prolonged healing, as seen in chronic wounds [10]. Increased levels of collagen secretion is also observed in keloidal and hypertrophic scar tissues, and are characterize by the formation of parallel collagen fibers [9]. Patients suffering from direct and indirect hernias had significantly higher collagen type III levels than those without hernias [20]. This could be either a consequence or instigation from abnormal angiogenesis at the injury site [20]. Surface modifications showing lower levels of collagen type III are potential treatments that could assist progression to the remodeling stage. As the wound healing process progresses, collagen III is steadily replaced with collagen I [44].

The composition of the collagen types secreted by stromal cells varies depending on the tissue location in the human body, thus type I collagen is more dominant in stiffer environments such as bones and tendons whereas type III dominates softer environments such as blood vessels and fascia [45]. Collagen III levels for the skin control (26 ± 7%) matched previously reported values [18]. Overlapping levels of collagen III signal to that of the skin control and previously conducted research, such as those measured for nitroarginine (36 ± 8%) and albizzin (42 ± 13%), could indicate possible progression of the wound healing process towards reepitheliazation [44,46]. The collagen III levels had no correlation with the FWHM of the collagen organization (R = 0.24). The estimated levels of collagen III varied greatly across the samples from 2 to 42%. Acute or chronic inflammatory responses to the implant can influence collagen III secretion [47].

Integrins are transmembrane receptors that facilitate ECM deposition, which is a key phase of the host response to naïve and functionalized surfaces [48,49]. A specific integrin, α2β1, has been observed on platelets, fibroblasts, and epithelial cells for its affinity to bind with

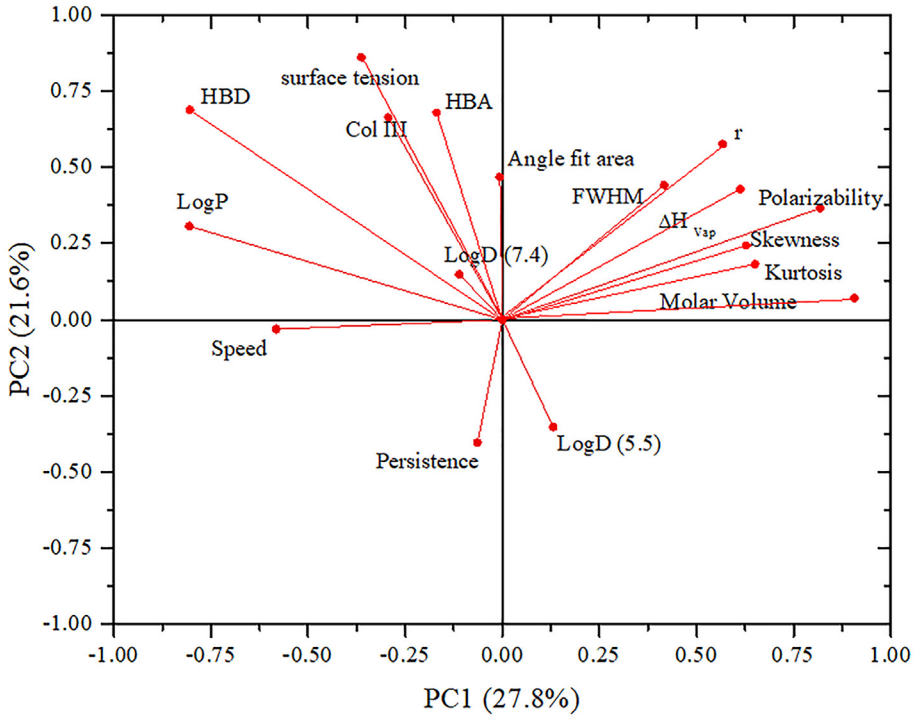

Fig. 6. Loading plot of physicochemical materials properties and their influence on cell mobility and collagen organization. PC1 explains 27.8% data variance and PC2 explains 21.6% data variance. HBD = hydrogen bond donors, HBA = hydrogen bond acceptors, r = freely rotating bonds.

collagen, which contains the GFOGER sequence [50]. It is possible that the arginine-like modifications studied here could be influencing the collagen deposition and organization [49,50] through a similar mechanism.

Surface properties play a major role in how secreted types of collagen coalesce to form different network meshes on varied substrates [51]. The hydrophobicity of functionalized polymer substrates has been studied for its influence on the adsorption of secreted collagen in the presence of different biological sera [52,53]. This link between hydrophobicity and collagen was further explored in a study in which terminal-group modified self-assembled monolayers of alkanethiols on gold were implanted in air pouches. The most hydrophobic surface coating of -CH_3 functionalized monolayers triggered the densest collagen secretion and fibrotic layer formation [54]. Previous studies on using diverse short and medium-chain fatty acid modifiers showed the significance of lipophilicity (logP) on the biological activity of Epstein-Barr virus, with a sensitivity to specific lipophilicity ranges of the fatty acid, where it was activated, inhibited and blocked for LogD ranges of -2.4 to 1.4, -1.0 to -0.3 and > 0, respectively [55]. These studies show the significant influence of the surface functionalization on the biological activity of the interacting cells, which we presume will influence the collagen organization as well as a part of the host response.

4.4. PCA

The physicochemical properties of different surface modifications can influence the cellular response of fibroblasts [24]. Informatics analysis of this data using PCA (Fig. 6) revealed correlations that can be used to explain relationships between chemical modifications and host responses to the implanted materials. Surface tension was well correlated with the collagen type III ratio surrounding the implant. It is important to note that the modifiers used here were relatively hydrophilic, with surface tensions ranging from 48 to 84 dyne/cm. Increased collagen III levels are essential in the earlier stages of wound healing. During later phases, collagen type III should be remodeled to collagen type I [56].

Larger FWHM values indicate isotropic collagen organization. Unwounded skin is isotropic [57]. It was observed from the PCA, that the collagen organization was closely correlated to the number of freely rotating bonds and the enthalpy of vaporization of the PLR modifications. However, the Pearson's correlations showed a negative correlation between the FWHM to the LogP ($R = -0.51$) and positive correlations to the surface tension and the number of freely rotating bonds ($R = 0.46$ and $R = 0.47$ respectively). Previous studies have shown that the number of freely rotating bonds could be linked with the secretion of tumor necrosis factor-α in both naïve and pro-inflammatory macrophages, through the interaction of macrophages with modified liposomes [58]. Another study showed how tuning the number of freely rotating bonds with a few other chemical structure parameters such as the number of carbon and hydrogen atoms can be used to promote an anti-inflammatory phenotype in macrophages interacting with PLR-modified poly(N-isopropylacrylamide)-*co*-acrylic acid microparticles [59]. This is of particular significance since anti-inflammatory macrophages are closely associated with the cell response pathways of transforming growth factor-β that are associated with instigation of collagen secretion by fibroblasts [60].

Kurtosis and skewness parameters are markers for collagen organization. Skewness is a measure of symmetry for the statistical distribution and kurtosis is a measure of whether the normal distribution is heavy or light-tailed. Together, these statistical parameters provide an analytical insight into the collagen organization beyond just the FWHM. In our study, we observed in the PCA (Fig. 6) that unlike the FWHM, the skewness and kurtosis were positively correlated to the polarizability and molar volume of the modifiers. Polarizability has been studied as a parameter in quantitative structure activity relationships (QSAR) analysis of diverse chemical structures influencing biological interactions such as nerve toxicity in frogs [61]. This influence of polarizability and its correlation through PCA to the fit parameters indicates that it could play a possible role in the alignment of collagen fibers as a part of biomaterial interactions with the host.

Intermolecular interactions resulting from differences in chemical structure can influence a variety of surface properties. The number of

HBDs, HBAs, and surface tension are closely linked to the hydrophobicity and surface charge of the functionalized substrate. Previous research on the hydrophobicity of surfaces showed that rat hepatocytes and schwannoma cells preferred hydrophobic surfaces with functionalized ECM proteins [53]. Clear differences have been observed for how MG-63 osteoblasts and NIH/3 T3 fibroblasts respond to hydrophilic and hydrophobic surfaces, with both cell types preferentially proliferating more on the hydrophobic surfaces [62]. A wide range of surface chemistries ranging from tissue culture polystyrene to oxidized silicon wafers were examined to measure the kinetics of surface sensing for the two cell types to different surface treatments. The NIH/3 T3 fibroblasts were more dynamic in their response to diverse surfaces compared to the osteoblasts, showing significant differences in proliferation from 2 to 5 days of culture even on highly hydrophilic substrates, as compared to the osteoblasts [62]. These studies have helped identify surface chemistries that can aid the biocompatibility of dental implant materials [63]. This link between surface hydrophobicity with cell adhesion and proliferation was explored in a study on cell responses to -CH_3, -COOH, and-NH_2 terminated surface assembled monolayers. Nealey et al. hypothesized that SV40 epithelial cell responses were influenced by the propensity of hydrophobic surfaces to promote protein deposition, as concurred by the previous study [62,64]. Considering the observations from the collagen organization and the collagen III levels together, the albizziin modification elicited the best collagen response under the *in vivo* conditions.

Altering the cell adhesion, migration, and proliferation on functionalized surfaces can improve wound healing and implant acceptance [65,66]. Modifying the underlying substrates with different ligand chemistries influences cell attachment and the subsequent production of ECM proteins that are integral aspects of the foreign body response [67]. Migration studies on these surfaces indicated that NIH/3 T3 fibroblasts migrated faster on creatine coated substrates [24]. In our SHG based analysis, we observed higher levels of collagen secretion and orientation in response to the creatine modified glass surface, which is in line with the aforementioned study. When the migration-based cell response parameters (*i.e.*, speed and persistence) were combined with the *ex vivo* SHG analysis and chemical properties in a PCA plot, we uncovered correlations with the chemical properties of the modifier. The negative Pearson's correlations for the speed with polarizability ($R = -0.53$) and molar volume ($R = -0.50$) were noted from the PCA, as possible influences on how the cell migration can be influenced by the surface charge and physical properties of the modifier (Table S1).

5. Conclusions

The collagen response to functionalized glass beads coated with modified PLRs was studied to better understand how chemical modifications can impact implant acceptance. Tissue sections were removed 28 days post-implantation and showed some significant differences in the measured collagen signal intensity, in particular for the creatine and albizziin modifications. Increased collagen type III had a positive correlation with hydrogen bond acceptors in the modifier structure and surface tension. PCA also uncovered correlations between the freely rotating bonds, and the enthalpy of vaporization of the modifier on the organization of collagen response to modified PLR coated glass beads. The insights obtained from correlating the chemical properties of the PLR modifications to the SHG imaging derived parameters can further the design principles for improving implant acceptance.

Supplementary data to this article can be found online at https://doi.org/10.1016/j.msec.2019.110143.

Acknowledgements

This work was supported by the National Science Foundation under Grant No. CBET-1227867 and the Roy J. Carver Charitable Trust Grant No. 13-4254. K.M.B. is grateful for the Michael and Denise Mack Faculty Fellowship.

References

[1] J.M. Anderson, A. Rodriguez, D.T. Chang, Foreign body reaction to biomaterials, Semin. Immunol. 20 (2008) 86–100.
[2] A.J. Singer, R. a F. Clark, Cutaneous wound healing, N. Engl. J. Med. 341 (1999) 738–746.
[3] R.A.F. Clark, Wound repair, Curr. Opin. Cell Biol. 1 (1989) 1000–1008.
[4] N.P. Ziats, K.M. Miller, J.M. Anderson, In vitro and in vivo interactions of cells with biomaterials, Biomaterials 9 (1988) 5–13.
[5] M. Kastellorizios, N. Tipnis, D.J. Burgess, Foreign body reaction to subcutaneous implants, Adv. Exp. Med. Biol. 865 (2015).
[6] D. Akilbekova, K.M. Bratlie, Quantitative characterization of collagen in the fibrotic capsule surrounding implanted polymeric microparticles through second harmonic generation imaging, PLoS One 10 (1–17) (2015).
[7] P. Martin, Wound healing–aiming for perfect skin regeneration, Science 276 (1997) 75–81 (80-.).
[8] J.A. Clark, J.C.Y. Cheng, K.S. Leung, Mechanical properties of normal skin and hypertrophic scars, Burns 22 (1996) 443–446.
[9] P.D.H.M. Verhaegen, et al., Differences in collagen architecture between keloid, hypertrophic scar, normotrophic scar, and normal skin: an objective histopathological analysis, Wound Repair Regen. 17 (2009) 649–656.
[10] K. Zhang, W. Garner, L. Cohen, J. Rodriguez, S. Phan, Increased types I and III collagen and transforming growth factor-β1 mRNA and protein in hypertrophic burn scar, J. Invest. Dermatol. 104 (1995) 750–754.
[11] P.P.M. Van Zuijlen, et al., Collagen morphology in human skin and scar tissue: no adaptations in response to mechanical loading at joints, Burns 29 (2003) 423–431.
[12] X. Chen, O. Nadiarynkh, S. Plotnikov, P.J. Campagnola, Second harmonic generation microscopy for quantitative analysis of collagen fibrillar structure, Nat. Protoc. 7 (2012) 654–669.
[13] P.J. Campagnola, L.M. Loew, Second-harmonic imaging microscopy for visualizing biomolecular arrays in cells, tissues and organisms, Nat Biotech 21 (2003) 1356–1360.
[14] J.L. Suhalim, et al., Characterization of cholesterol crystals in atherosclerotic plaques using stimulated Raman scattering and second-harmonic generation microscopy, Biophys. J. 102 (2012) 1988–1995.
[15] S.V. Plotnikov, A.C. Millard, P.J. Campagnola, W. Mohler, Characterization of the myosin-based source for second-harmonic generation from muscle sarcomeres, Biophys. J. 90 (2006) 693–703.
[16] A. Boddupalli, K.M. Bratlie, Multimodal imaging of harmonophores and application of high content imaging for early cancer detection, Mater. Discov. 1 (2015) 10–20.
[17] P.J. Su, et al., The discrimination of type I and type II collagen and the label-free imaging of engineered cartilage tissue, Biomaterials 31 (2010) 9415–9421.
[18] A.J. Bailey, T.J. Sims, M. Le Lous, S. Bazin, Collagen polymorphism in experimental granulation tissue, Biochem. Biophys. Res. Commun. 66 (1975) 1160–1165.
[19] S. Koruth, Y.V. Narayanaswamy Chetty, Hernias- is it a primary defect or a systemic disorder? Role of collagen III in all hernias- a case control study, Ann. Med. Surg. 19 (2017) 37–40.
[20] U. Klinge, et al., Synthesis of type I and III collagen, expression of fibronectin and matrix metalloproteinase 1 and 13 in hernias of patients with inguinal hernia, Int J Surg Invest 1 (1999) 219–227.
[21] G. Gabbiani, M. Le Lous, A.J. Bailey, A.S.B. Delaunay, Collagen and myofibroblasts of granulation tissue a chemical, ultrastructural and immunologic study, Virchows Arch. B Cell Path. 21 (1976) 133–145.
[22] Palero, J. A., de Bruijn, H. S., van der Ploeg van den Heuvel, A., Sterenborg, H. J. C. M. & Gerritsen, H. C. Spectrally resolved multiphoton imaging of in vivo and excised mouse skin tissues. Biophys. J.. 93, 992–1007 (2007).
[23] H.C. Bygd, K.D. Forsmark, K.M. Bratlie, Altering invivo macrophage responses with modified polymer properties, Biomaterials 56 (2015).
[24] H.C. Bygd, D. Akilbekova, A. Muñoz, K.D. Forsmark, K.M. Bratlie, Poly-l-arginine based materials as instructive substrates for fibroblast synthesis of collagen, Biomaterials 63 (2015) 47–57.
[25] J.E. Albina, et al., Arginine metabolism in wounds, Am. J. Physiol. Metab. 254 (1988) E459–E467.
[26] J.E. Albina, M.D. Caldwell, W.L. Henry, C.D. Mills, Regulation of macrophage functions by L-arginine, J. Exp. Med. 169 (1989) 1021–1029.
[27] L.A. Norian, et al., Tumor-infiltrating regulatory dendritic cells inhibit CD8+ T cell function via L-arginine metabolism, Cancer Res. 69 (2009) 3086–3094.
[28] J.D. Shearer, J.R. Richards, C.D. Mills, M.D. Caldwell, Differential regulation of macrophage arginine metabolism: a proposed role in wound healing, Am. J. Physiol. Metab. 272 (1997) E181–E190.
[29] V. Bronte, P. Zanovello, Regulation of immune responses by L-arginine metabolism, Nat. Rev. Immunol. (8) (2005) 641–656.
[30] T. Arimoto, G. Bing, Up-regulation of inducible nitric oxide synthase in the substantia nigra by lipopolysaccharide causes microglial activation and neurodegeneration, Neurobiol. Dis. 12 (2003) 35–45.
[31] V. Calabrese, et al., Disruption of thiol homeostasis and nitrosative stress in the cerebrospinal fluid of patients with active multiple sclerosis: evidence for a protective role of acetylcarnitine, Neurochem. Res. 28 (2003) 1321–1328.
[32] S. Shin, et al., Simultaneous analysis of acetylcarnitine, proline, hydroxyproline, citrulline, and arginine as potential plasma biomarkers to evaluate NSAIDs-induced gastric injury by liquid chromatography–tandem mass spectrometry, J. Pharm. Biomed. Anal. 165 (2019) 101–111.
[33] H.P. Gavin, The Levenberg-Marquardt Method for Nonlinear Least Squares Curve-

fitting Problems, Department of Civil and Environmental Engineering, Duke University, 2013.
[34] G.S. Ashcroft, et al., Mice lacking Smad3 show accelerated wound healing and an impaired local inflammatory response, Nat. Cell Biol. 1 (1999) 260–266.
[35] V. Ajeti, et al., Structural changes in mixed Col I/Col V collagen gels probed by SHG microscopy: implications for probing stromal alterations in human breast cancer, Biomed. Opt. Express 2 (2011) 2307–2316.
[36] A. Knott, et al., A novel treatment option for photoaged skin, J. Cosmet. Dermatol. 7 (2008) 15–22.
[37] F. Fischer, et al., Folic acid and creatine improve the firmness of human skin in vivo, J. Cosmet. Dermatol. 10 (2011) 15–23.
[38] L. Gailhouste, et al., Fibrillar collagen scoring by second harmonic microscopy: a new tool in the assessment of liver fibrosis, J. Hepatol. 52 (2010) 398–406.
[39] H.A. Linares, C.W. Kischer, M. Dobrkovsky, D.L. Larson, The histotypic organization of collagen of the hypertrophic scar in humans, J. Invest. Dermatol. 59 (1972) 323–332.
[40] H.P. Ehrlich, et al., Morphological and immunochemical differences between keloid and hypertrophic scar, Am. J. Pathol. 145 (1994) 105–113.
[41] T. Yasui, Y. Tohno, T. Araki, Characterization of collagen orientation in human dermis by two-dimensional second-harmonic-generation polarimetry, J. Biomed. Opt. 9 (2004) 259–264.
[42] H. Martínez, C. Brackmann, A. Enejder, P. Gatenholm, Mechanical stimulation of fibroblasts in micro-channeled bacterial cellulose scaffolds enhances production of oriented collagen fibers, J. Biomed. Mater. Res. - Part A 100 A (2012) 948–957.
[43] M. Olderøy, et al., Biochemical and structural characterization of neocartilage formed by mesenchymal stem cells in alginate hydrogels, PLoS One 9 (2014).
[44] S.W. Volk, Y. Wang, E. a Mauldin, K.W. Liechty, S.L. Adams, Diminished type III collagen promotes myofibroblast differentiation and increases scar deposition in cutaneous wound healing, Cells Tissues Organs 194 (2011) 25–37.
[45] M.C. Robson, D.L. Steed, M.G. Franz, Wound healing: biologic features and approaches to maximize healing trajectories, Curr. Probl. Surg. 38 (1–140) (2001).
[46] B.K. Brisson, et al., Type III collagen directs stromal organization and limits metastasis in a murine model of breast cancer, Am. J. Pathol. 185 (2015) 1471–1486.
[47] J.N. Clore, I.K. Cohen, R.F. Diegelmann, Quantitation of collagen types I and III during wound healing in rat skin, Proc. Soc. Exp. Biol. Med. 161 (1979) 337–340.
[48] C. Gaudet, et al., Influence of type I collagen surface density on fibroblast spreading, motility, and contractility, Biophys. J. 85 (2003) 3329–3335.
[49] C. Zeltz, D. Gullberg, The integrin-collagen connection - a glue for tissue repair? J. Cell Sci. 129 (2016) 653–664.
[50] J. Emsley, C.G. Knight, R.W. Farndale, M.J. Barnes, R.C. Liddington, Structural basis of collagen recognition by integrin α2β1, Cell 101 (2000) 47–56.
[51] B.N. Brown, et al., Surface characterization of extracellular matrix scaffolds, Biomaterials 31 (2010) 428–437.
[52] J. Dewez, V. Berger, Y. Schneider, P. Rouxhet, Influence of substrate hydrophobicity on the adsorption of collagen in the presence of pluronic F68, albumin, or calf serum, J. Colloid Interface Sci. 191 (1997) 1–10.
[53] J.L. Dewez, et al., Adhesion of mammalian cells to polymer surfaces: from physical chemistry of surfaces to selective adhesion on defined patterns, Biomaterials 19 (1998) 1441–1445.
[54] J.N. Barbosa, P. Madureira, M.A. Barbosa, A.P. Águas, The influence of functional groups of self-assembled monolayers on fibrous capsule formation and cell recruitment, J. Biomed. Mater. Res. - Part A 76 (2006) 737–743.
[55] K.L. Gorres, D. Daigle, S. Mohanram, G. Miller, Activation and repression of Epstein-Barr virus and Kaposi's sarcoma-associated herpesvirus lytic cycles by short- and medium-chain fatty acids, J. Virol. 88 (2014) 8028–8044.
[56] H.N. Lovvorn, et al., Relative distribution and crosslinking of collagen distinguish fetal from adult sheep wound repair, J. Pediatr. Surg. 34 (1999) 218–223.
[57] R. Cicchi, et al., Scoring of collagen organization in healthy and diseased human dermis by multiphoton microscopy, J. Biophotonics 3 (2010) 34–43.
[58] H.C. Bygd, L. Ma, K.M. Bratlie, Physicochemical properties of liposomal modifiers that shift macrophage phenotype, Mater. Sci. Eng. C 79 (2017) 237–244.
[59] A.J. Dunn-sale, K.M. Bratlie, Identifying factors of microparticles modified with arginine derivatives that induce phenotypic shifts in macrophages, ACS Biomater. Sci. Eng. 2 (1–25) (2016).
[60] R.K. Assoian, et al., Expression and secretion of type beta transforming growth factor by activated human macrophages, Proc. Natl. Acad. Sci. U. S. A. 84 (1987) 6020–6024.
[61] C. Hansch, et al., On the role of polarizability in chemical - biological interactions, J. Chem. Inf. Comput. Sci. 43 (2003) 120–125.
[62] H. Schweikl, et al., Proliferation of osteoblasts and fibroblasts on model surfaces of varying roughness and surface chemistry, J. Mater. Sci. Mater. Med. 18 (2007) 1895–1905.
[63] G. Schmalz, Strategies to improve biocompatibility of dental materials, Curr. Oral Heal. Reports 1 (2014) 222–231.
[64] M. Franco, P.F. Nealey, S. Campbell, A.I. Teixeira, C.J. Murphy, Adhesion and proliferation of corneal epithelial cells on self-assembled monolayers, J. Biomed. Mater. Res. 52 (2000) 261–269.
[65] B.K. Mann, J.L. West, Cell adhesion peptides alter smooth muscle cell adhesion, proliferation, migration, and matrix protein synthesis on modified surfaces and in polymer scaffolds, J. Biomed. Mater. Res. 60 (2002) 86–93.
[66] Z. Yang, et al., Bioactive plasma-polymerized bipolar films for enhanced endothelial cell mobility, Macromol. Biosci. 11 (2011) 797–805.
[67] L. Marinucci, et al., Biocompatibility of collagen membranes crosslinked with glutaraldehyde or diphenylphosphoryl azide: an in vitro study, J. Biomed. Mater. Res. A 67 (2003) 504–509.